

Space Charge Limit and Mitigation Approaches in Synchrotrons

Adrian Oeftiger

Space Charge Workshop ORNL, USA
24 October 2022

Motivation

Facility for Antiproton and Ion Research

- SIS100: deliver high-intensity beams

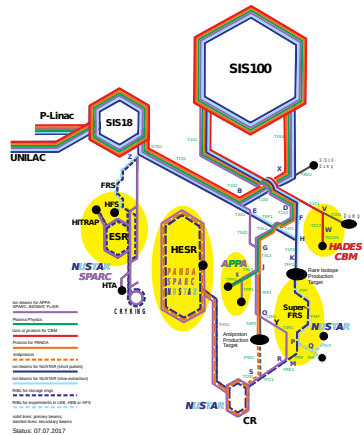


Figure: FAIR complex

Motivation

Facility for Antiproton and Ion Research

- SIS100: deliver high-intensity beams
- crucial for performance: maintain beam quality during 1-sec injection plateau
- uranium U^{28+} beam most critical:
 - largest beam size vs. transverse aperture
 - space-charge induced losses
 - ~~ dynamic vacuum issues
 - ==> low-loss operation < 5%!
- key question:
what is the space-charge limit?

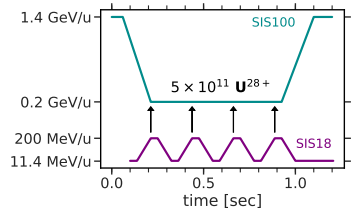


Figure: SIS18 to SIS100 transfer

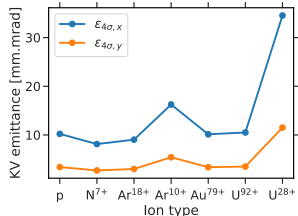


Figure: scaled beam sizes at 18 Tm

PHYSICAL REVIEW ACCELERATORS AND BEAMS **25**, 054402 (2022)

Simulation study of the space charge limit in heavy-ion synchrotrons

Adrian Oeftiger^{1,*}, Oliver Boine-Frankenheim^{1,2}, Vera Chetvertkova¹,
Vladimir Kornilov¹,[!] Dmitry Rabusov²,[!] and Stefan Sorge¹

¹GSI Helmholtzzentrum für Schwerionenforschung GmbH, Planckstrasse 1, 64291 Darmstadt, Germany

²Technische Universität Darmstadt, Schlossgartenstrasse 8, 64289 Darmstadt, Germany

(Received 5 November 2021; accepted 6 April 2022; published 16 May 2022)

Key ingredients of study:

1. detailed model for **magnetic field errors** from cold bench measurements
2. **full tracking model** of machine lattice
3. detailed **space charge** models
 - self-consistent 3D PIC solver (particle-in-cell)
 - fast (approximative) frozen field maps

⇒ parallelised on multi-core CPU and GPU architectures

PHYSICAL REVIEW ACCELERATORS AND BEAMS **25**, 054402 (2022)

Simulation study of the space charge limit in heavy-ion synchrotrons

Adrian Oeftiger^{1,*}, Oliver Boine-Frankenheim^{1,2}, Vera Chetvertkova¹,
Vladimir Kornilov¹,[!] Dmitry Rabusov²,[!] and Stefan Sorge¹

¹GSI Helmholtzzentrum für Schwerionenforschung GmbH, Planckstrasse 1, 64291 Darmstadt, Germany

²Technische Universität Darmstadt, Schlossgartenstrasse 8, 64289 Darmstadt, Germany

(Received 5 November 2021; accepted 6 April 2022; published 16 May 2022)

Structure:

A. The Model

B. Betatron Resonances:

- Intrinsic from Space Charge
- External from Field Errors

C. Space-Charge Limit

D. Mitigation Measures

A. The Model

Simulation model:

- track macro-particles (m.p.) through accelerator lattice & space charge kicks
- nonlinear 3D space charge (SC) models:
 - self-consistent **PIC**: particle-in-cell for open-boundary Poisson equation
 - fixed frozen (**FFSC**): constant field map independent of m.p. dynamics
 - (adaptive frozen (**AFSC**): field map scaled with m.p. distribution momenta)

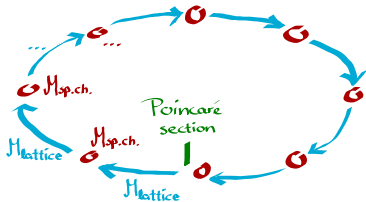


Figure: sketch of simulation model

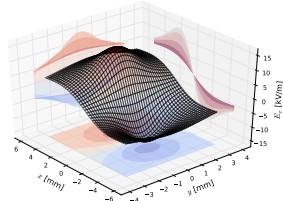


Figure: horizontal space charge field

Simulation model:

- track macro-particles (m.p.) through accelerator lattice & space charge kicks
- nonlinear 3D space charge (SC) models:
 - *self-consistent PIC*: particle-in-cell for open-boundary Poisson equation
 - *fixed frozen (FFSC)*: constant field map independent of m.p. dynamics

Maximum SC Tune Shift

$$\Delta Q_y^{\text{SC}} = -\frac{Ze}{4\pi\epsilon_0 m_0 c^2} \frac{\lambda_{\max}}{\beta^2 \gamma^3} \frac{1}{2\pi} \oint ds \frac{\beta_y(s)}{\sigma_y(s)(\sigma_x(s) + \sigma_y(s))}$$



Figure: sketch of simulation model

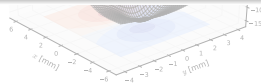


Figure: horizontal space charge field

Beam Parameters

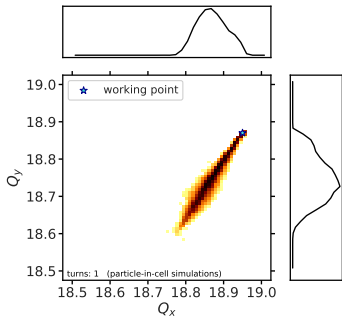


Figure: space charge tune footprint

Table: Considered Parameters for $^{238}\text{U}^{28+}$ Accumulation at SIS100 Injection Energy

Parameter	Value
Hor. norm. rms emittance ϵ_x	5.9 mm mrad
Vert. norm. rms emittance ϵ_y	2.5 mm mrad
Rms bunch length σ_z	13.2 m
Bunch intensity N_0 of U^{28+} ions	0.625×10^{11}
Max. space charge $\Delta Q_{\text{y}}^{\text{SC}}$	-0.30
Rms chromatic $Q'_{x,y} \cdot \sigma_{\Delta p/p_0}$	0.01
Synchrotron tune Q_s	4.5×10^{-3}
Kinetic energy	$E_{\text{kin}} = 200 \text{ MeV/u}$
Relativistic β factor	0.568
Revolution frequency f_{rev}	157 kHz

B. Betatron Resonances

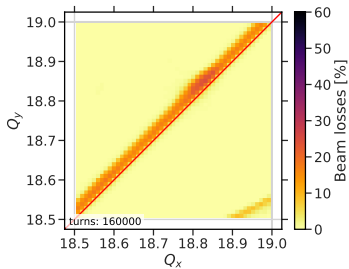


Figure: tune diagram of beam loss

Cold, error-free, symmetric SIS100 lattice:

- perfect dipole and quadrupole magnets
- symmetry of $S = 6$ maintained
(no warm / normalconducting quadrupoles)
- space charge → only source for resonances
- simulated for 160'000 turns = 1 second
- ⇒ mainly Montague resonance visible
- ⇒ absence of low-order structure resonances!

Only Space Charge

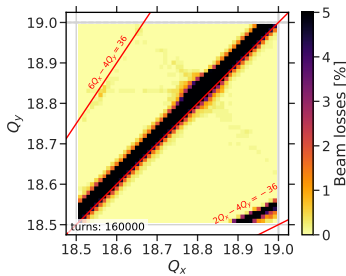


Figure: tune diagram of beam loss

Cold, error-free, symmetric SIS100 lattice:

- perfect dipole and quadrupole magnets
- symmetry of $S = 6$ maintained
(no warm / normalconducting quadrupoles)
- space charge → only source for resonances
- simulated for 160'000 turns = 1 second
- ⇒ mainly Montague resonance visible
- ⇒ absence of low-order structure resonances!

Montague Resonance

Montague resonance $2Q_x - 2Q_y = 0$:

- 4th-order resonance
- intrinsically driven by space charge
- transverse emittance exchange for anisotropic beams
- ➡ stopband always present around $Q_x \approx Q_y$ for SIS100 beams

Space charge model predictions:

- **bad:** “adaptive frozen” resolves full exchange but predicts too large stopband extent
- + **good:** “fixed frozen” resolves stopband edges well!

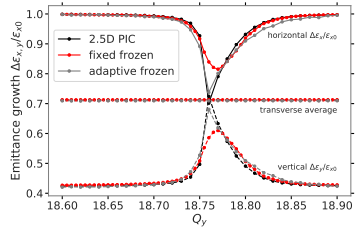


Figure: emittance exchange

Montague resonance $2Q_x - 2Q_y = 0$:

- 4th-order resonance
 - intrinsically driven by space charge
 - transverse emittance exchange for anisotropy
- ⇒ stopband for “Fixed frozen” model better suited than “adaptive frozen” to approximate realistic PIC when **identifying loss-free conditions!**

Observation



Space charge model predictions:

- bad: “adaptive frozen” resolves full exchange but predicts too large stopband extent
- + good: “fixed frozen” resolves stopband edges well!

Figure: emittance exchange

Warm Quadrupoles

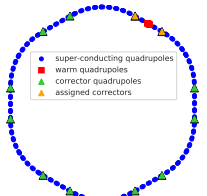


Figure: SIS100 quadrupole survey

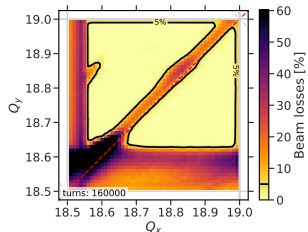


Figure: corrected warm quadrupoles

Real SIS100 lattice:

- 2 cold quadrupoles replaced by warm / normalconducting quadrupoles (radiation hardened, required in extraction region)
- breaking of $S = 6$ symmetry
 - ⇒ gradient error
 - ⇒ externally driven half-integer resonance
 - ⇒ can be minimised by quadrupole correctors

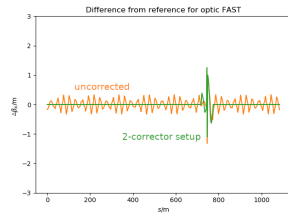


Figure: β -beat around SIS100 [courtesy D. Ondreka]

Half-integer Resonance

Half-integer stopband:

- without space charge, without $\Delta p/p_0$: $\delta Q_{\text{stopband}} = 0.023$
 - without space charge, with $\Delta p/p_0$: $\delta Q_{\text{stopband}} \sim 0.1$
 - with space charge: $\delta Q_{\text{stopband}} \sim 0.25$
- ⇒ fixed frozen SC model reproduces stopband edges from PIC

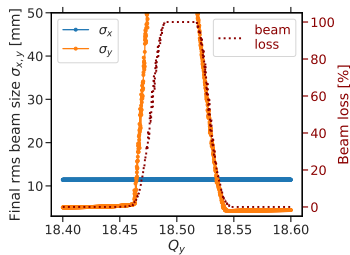


Figure: no space charge

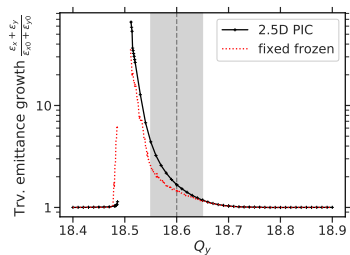


Figure: with space charge

Field Error Model

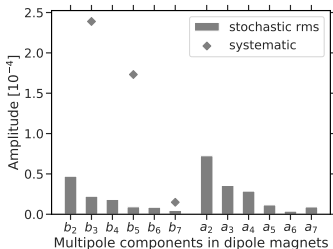


Figure: dipole magnets

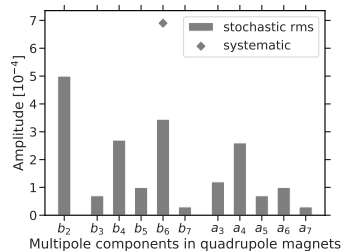


Figure: quadrupole magnets

Field error model extracted from cold bench measurements of magnet units:

- stochastic amplitudes drive non-systematic resonances
- random number sequence → multipole errors for every dipole and quadrupole magnet

quadrupole model displayed here corresponds to PRAB paper version (based on stamped FoS),
see GSI-2021-00450 report / for model based on series production and its comparison

Full Model with Space Charge

Linear and nonlinear resonances driven by magnet field errors. Resonance condition without space charge:

$$mQ_x + nQ_y = p \quad \text{for } m, n, p \in \mathbb{Z}$$

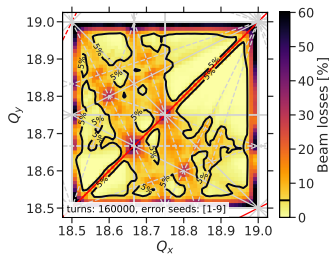


Figure: no space charge

include
SC

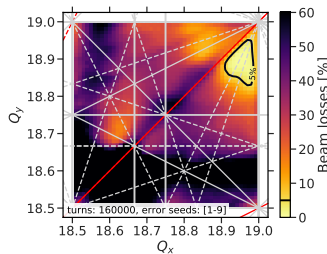


Figure: with fixed frozen space charge

- SC broadens existing resonance stopbands
- optimal working point area around $(Q_x, Q_y) = (18.95, 18.87)$
[requires transverse feedback system to fight resistive wall instability!]

Validation with Self-consistent PIC

Self-consistent PIC simulations:

- ✓ validated Montague resonance
- ✓ validated half-integer resonance
- now validate full error model FFSC predictions for beam loss

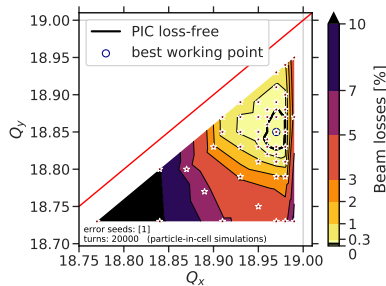


Figure: self-consistent PIC simulations

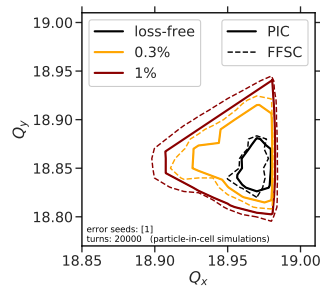


Figure: comparison between SC models

note: PIC simulations take 2 days (on NVIDIA V100 GPU) vs. FFSC simulations with 7 min (on 16 CPU cores, HPC AMD)

Relevant Field Error Orders

Major resonances confining low-loss area:

- top left: Montague resonance
- right: integer resonance $Q_x = 19$
- bottom: higher-order resonances

Simulations with reduced field error model:

- identify sextupole and octupole orders $n=3,4$ as main limitation towards low Q_y

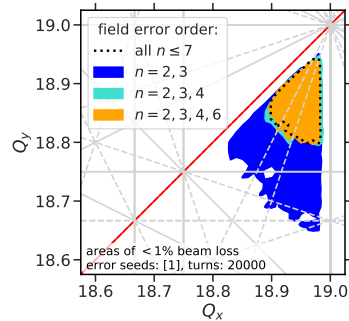
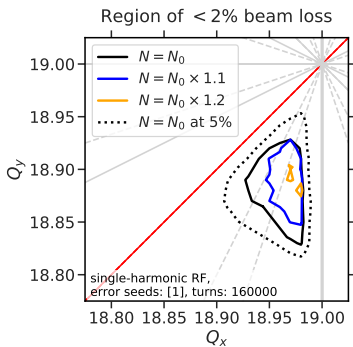


Figure: low-loss tune areas vs. multipole order

C. Space-Charge Limit

dynamic definition of space-charge limit

reached when loss-free working point area vanishes



Keeping all beam parameters identical,
increasing N :

⇒ U^{28+} space-charge limit at **120%** of
nominal bunch intensity N_0 :

$$\max |\Delta Q_y^{\text{SC}}| = 0.36$$

Figure: low-loss area for increasing N

D. Mitigation Measures

Correction of β -beat

Two sources of β -beat (gradient error):

- warm quadrupoles: uncorrected = 2%
 - significant effect on low-loss area size
 - important to control

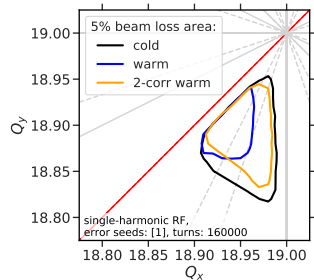


Figure: low-loss area with warm quadrupoles

Correction of β -beat



Two sources of β -beat (gradient error):

- warm quadrupoles: uncorrected = 2%
 - significant effect on low-loss area size
 - important to control
- distributed b_2 : $\approx 0.5\%$
(according to field error model)
 - below $b_2 = 10$ units:
no significant effect on low-loss area size

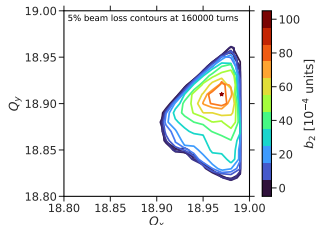


Figure: low-loss area with b_2

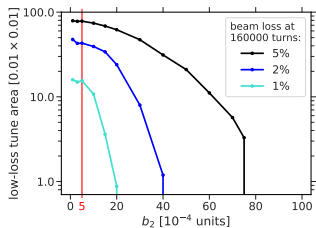


Figure: size of low-loss area vs. b_2

Double-harmonic RF

By adding $h = 20$ harmonic at half base RF voltage in bunch lengthening mode,

$$V_{h=20} = V_{h=10}/2$$

obtain flattened bunches with reduced line charge density at 80% of nominal λ_{\max} .

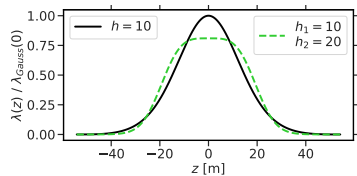


Figure: line densities

Results with Double-harmonic RF

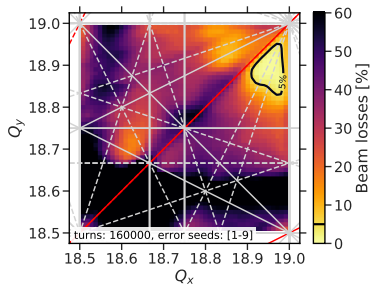


Figure: single-harmonic RF

flatten
↔
bunch

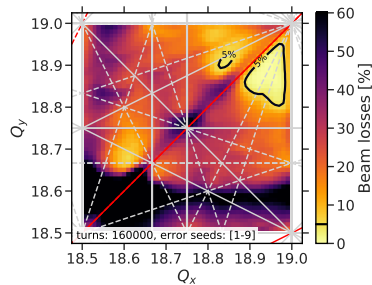


Figure: double-harmonic RF

Observations:

- black half-integer stopband shrinks by $\approx 20\%$
- low-loss area opens up

Increasing N for double-harmonic RF:

- find space-charge limit at **150%** of nominal intensity N_0

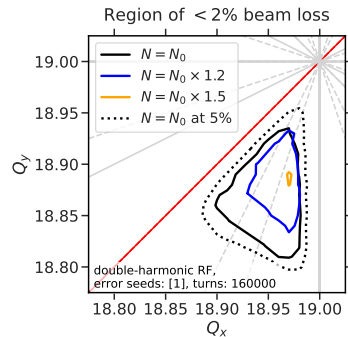


Figure: low-loss area for increasing N

Pulsed Electron Lenses

Pulsed electron lenses:

- short insertion with co-propagating electron beam
- transversely homogeneous distribution
- longitudinally modulated to match ion bunch profile
- compensate longitudinal dependency of space charge
(ideal: half compensation of linear space charge tune shift, $\Delta Q_{\text{elens}} = \Delta Q_{\text{KV}}/2$)
- ⇒ installing 3 such electron lenses shrinks stopbands!
- ⇒ space-charge limit increased significantly!

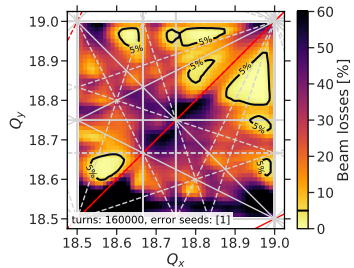


Figure: tune diagram at nominal N

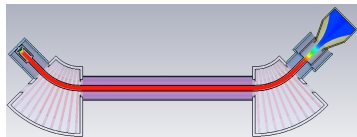


Figure: e-lens model for SIS18

Pulsed Electron Lenses

Pulsed electron lenses:

- short insertion with co-propagating electron beam
- transversely homogeneous distribution
- longitudinally modulated to match ion bunch profile
- compensate longitudinal dependency of space charge
(ideal: half compensation of linear space charge tune shift, $\Delta Q_{\text{elens}} = \Delta Q_{\text{KV}}/2$)
- ⇒ installing 3 such electron lenses shrinks stopbands!
- ⇒ space-charge limit increased significantly!

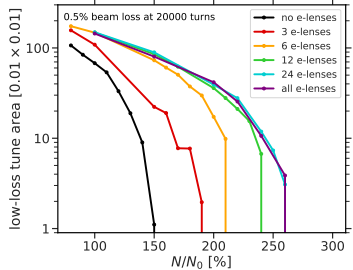


Figure: low-loss area for increasing N
[preliminary, unpublished results]

Conclusion

Summary:

- **validated** fixed frozen SC model predictions by long-term PIC simulations
- identified **optimal tune area** around $(Q_x, Q_y) = (18.95, 18.87)$
 - rigid constraints: Montague resonance (top left), integer resonance (right)
 - soft constraint: higher-order resonances (bottom)
- explored **space-charge limit**: $\max |\Delta Q_y^{\text{SC}}| = 0.36$
 - nominal SIS100: +20% intensity
 - double-harmonic RF: +50% intensity
 - 3 pulsed electron lenses: +80..90% intensity

take-home message

- dynamic space-charge limit: find based on tolerable loss & emittance growth
- nominal FAIR intensity → feasibility confirmed

Next steps:

- coherent stability with space charge (resistive-wall, nonlinear electron lenses)
- quantify impact by indirect space charge

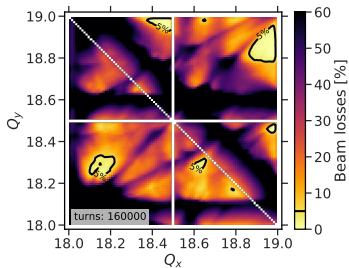


Figure: GPU simulation results for latest magnet field error model

Thanks to GSI's new high-performance GPU cluster in Green Cube:

- 400 GPU cards of today's most performant model (AMD Radeon Instinct MI100)
- even faster simulations, larger tune scans in shorter times
- ⇒ following up magnet series production and doublet assembly

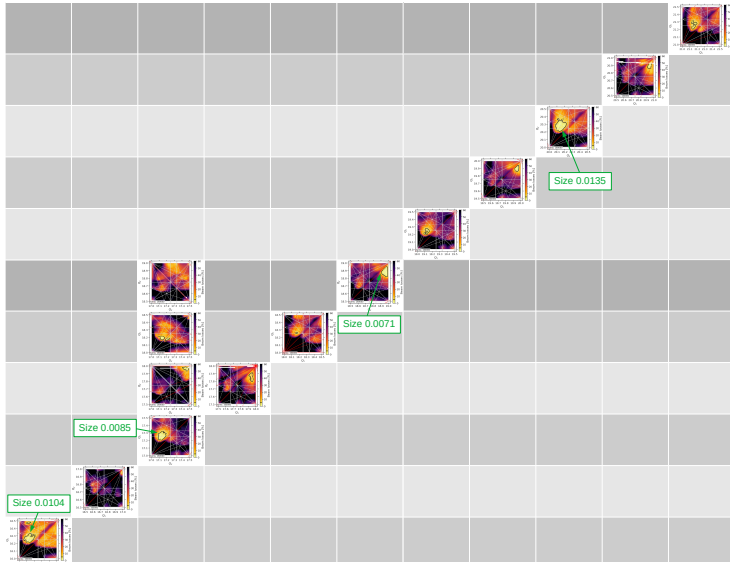
Thank you for your attention!

Acknowledgements:

GSI: O. Boine-Frankenheim, V. Chetvertkova, V. Kornilov, D. Rabusov, S. Sorge,
D. Ondreka, A. Bleile, V. Maroussov, C. Roux, K. Sugita

CERN: R. de Maria, G. Iadarola, M. Schwinzerl

Grand Overview Tune Diagrams



Emittance Growth at Low-loss Area

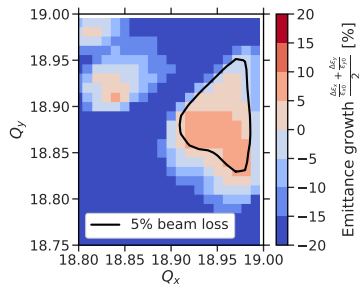


Figure: with space charge, emittance growth

PIC Results for Best Working Point

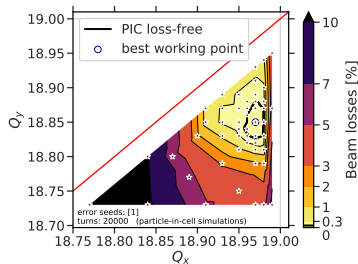


Figure: tune diagram with self-consistent PIC simulations

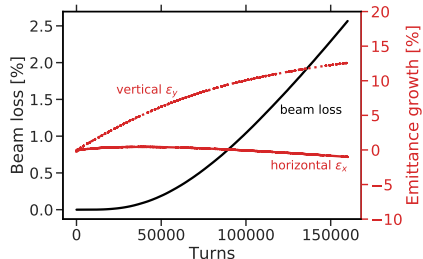


Figure: optimal working point
 $(Q_x, Q_y) = (18.97, 18.85)$

Comparison 2.5D to 3D PIC

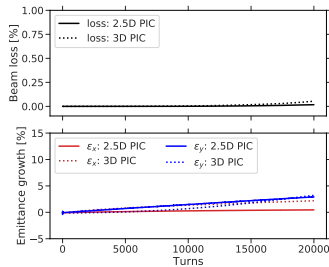


Figure: good working point (Q_x, Q_y) = (18.97, 18.85)

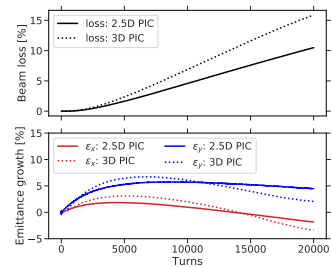
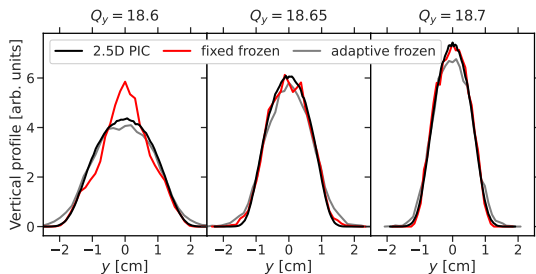


Figure: lossy working point (Q_x, Q_y) = (18.84, 18.73)

Adaptive Frozen SC Model



Half-integer Resonance vs. SC

Nuclear Inst. and Methods in Physics Research, A 1040 (2022) 167290



Characterization and minimization of the half-integer stop band with space charge in a hadron synchrotron

Dmitrii Rabusov ^{a,*}, Adrian Oeftiger ^b, Oliver Boine-Frankenheim ^{a,b}

^a Technische Universität Darmstadt, Schlossgartenstr. 8, 64289 Darmstadt, Germany

^b GSI Helmholtzzentrum für Schwerionenforschung GmbH, Planckstr. 1, 64291 Darmstadt, Germany

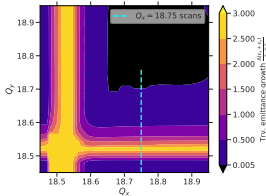


Figure: emittance growth in 2D tune diagram

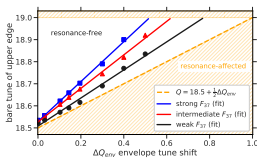


Figure: space-charge limit for Gaussian bunches

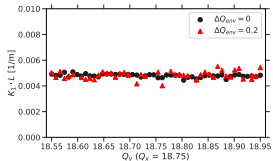


Figure: correction independent of space charge

Half-integer Resonance vs. SC

Nuclear Inst. and Methods in Physics Research, A 1040 (2022) 167290



Contents lists available at ScienceDirect

Nuclear Inst. and Methods in Physics Research, A

journal homepage: www.elsevier.com/locate/nima



Characterization and minimization of the half-integer stop band with space charge in a hadron synchrotron



Dmitrii Rabusov ^{a,*}, Adrian Oeftiger ^b, Oliver Boine-Frankenheim ^{a,b}

^a Technische Universität Darmstadt, Schlossgartenstr. 8, 64289 Darmstadt, Germany

^b GSI Helmholtzzentrum für Schwerionenforschung GmbH, Planckstr. 1, 64291 Darmstadt, Germany

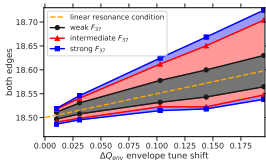


Figure: coasting beam stopband edges vs. space charge

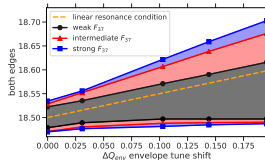


Figure: bunched beam stopband edges vs. space charge

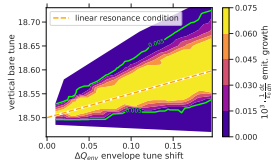


Figure: choose a threshold